ACS SENSORS

Article

Cite This: ACS Sens. 2017, 2, 1539-1545

pubs.acs.org/acssensors

Optimizing Stem Length To Improve Ligand Selectivity in a Structure-Switching Cocaine-Binding Aptamer

Miguel A. D. Neves,[‡] Aron A. Shoara,[‡] Oren Reinstein,[‡] Okty Abbasi Borhani, Taylor R. Martin, and Philip E. Johnson*

Department of Chemistry and Centre for Research on Biomolecular Interactions, York University, Toronto, Ontario M3J 1P3, Canada

Supporting Information

ABSTRACT: Understanding how aptamer structure and function are related is crucial in the design and development of aptamer-based biosensors. We have analyzed a series of cocaine-binding aptamers with different lengths of their stem 1 in order to understand the role that this stem plays in the ligand-induced structure-switching binding mechanism utilized in many of the sensor applications of this aptamer. In the cocaine-binding aptamer, the length of stem 1 controls whether the structure-switching binding mechanism for this aptamer occurs or not. We varied the length of stem 1 from being one to seven base pairs long and found that the structural transition from unfolded to folded in the unbound aptamer is when the aptamer elongates from 3 to 4 base pairs in stem 1. We then used this knowledge to achieve new binding selectivity of this aptamer for quinine over cocaine by using an aptamer with a stem 1 two base pairs long. This selectivity is achieved by means of the greater affinity quinine has for the aptamer compared with cocaine. Quinine provides enough free energy to both fold and bind the 2-base pair-long aptamer while cocaine does not. This tuning of binding selectivity of an aptamer by reducing its stability is likely a general mechanism that could be used to tune aptamer specificity for tighter binding ligands.

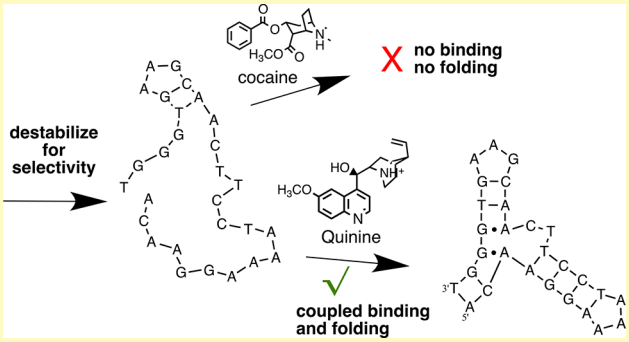

KEYWORDS: *biosensor, cocaine-binding aptamer, aptamer design, ligand binding thermodynamics, coupled folding and binding*

The development of aptamer-based sensing technologies is a rapidly growing field. Reasons for this include the ease of current *in vitro* selection strategies that can select an aptamer for almost any target and the straightforward nature of nucleic acid chemical modifications that allow for the easy immobilization of an aptamer to a sensing surface or covalent attachment of a chemical label or tag.[1−4] Many aptamers undergo or can be engineered to undergo a structural transition upon ligand binding, and the signal transduction schemes of many aptamer-based biosensors require ligand-induced structural changes or structure formation of the aptameric probe.[1,2,5−7] In general, structure-switching aptamers have lower affinity for their targets than aptamers that feature a preformed secondary structure. However, biosensors that can function using either a structure-switching or a rigid aptamer display greater analytical sensitivity using the structure-switching aptamer, despite the lower affinity.[8,9] This indicates that, in general, the structural changes that an aptamer undergoes upon ligand binding are more important for ligand selectivity than just the affinity of the aptamer when utilized as the biosensing element in a sensor provided sufficient affinity is retained by the aptamer.

The cocaine-binding aptamer has become a model system for the evaluation of novel and proof-of-concept small-molecule biosensors.[10−14] Structurally, the cocaine-binding aptamer comprises a three-way junction that contains a two-nucleotide bulge at the junction and a tandem AG mismatch (Figure 1).[15] When stem 1 is six base pairs long, the aptamer is structured in the free state and retains the same secondary structure in the bound state.[15] In contrast, when stem 1 is three base pairs long, the aptamer is unstructured or loosely structured and becomes structured when ligand-bound.[11,15−17] This structure formation process is analogous to the function of intrinsically disordered proteins in having coupled folding and binding.[18−20] As is the case with many aptamer based sensors, the majority of cocaine-binding aptamer biosensors utilize the structure switching sequence variant to generate adequate signal transduction, and this has contributed to the cocaine-binding aptamer becoming one of the most widely utilized aptamer model systems to evaluate small-molecule biosensing technologies.[9,11,12,21−26]

Unusually, the cocaine-binding aptamer binds quinine approximately 50-fold tighter than cocaine, the ligand that the aptamer was originally selected to bind.[27−30] The aptamer has two separate binding sites with ligand binding at the lower affinity site dependent on the NaCl concentration. At NaCl

Received: August 29, 2017
Accepted: September 20, 2017
Published: September 20, 2017

DOI: 10.1021/acssensors.7b00619
ACS Sens. 2017, 2, 1539−1545

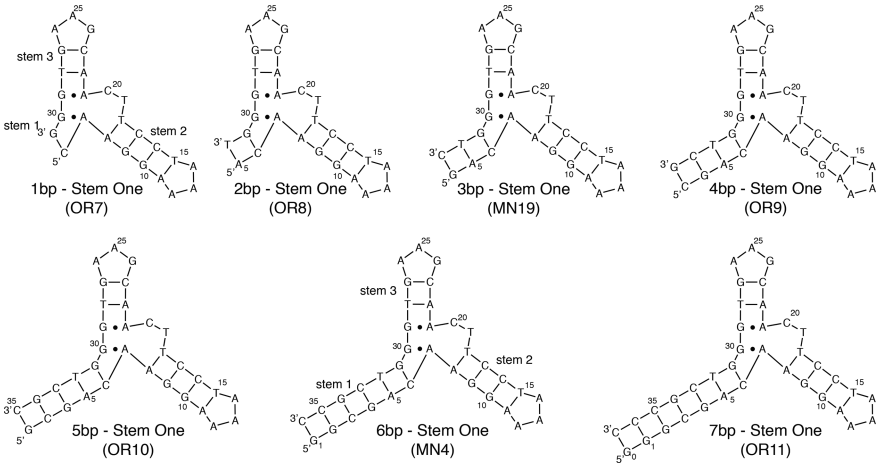

Figure 1. Sequence and secondary structures of cocaine-binding aptamers investigated in this study. For ease of comparison, nucleotides in all constructs are numbered in the same manner.

concentrations of ~50 mM or lower, two cocaine or quinine molecules bind with a two independent site binding mechanism. At higher NaCl concentrations only one copy of cocaine or quinine is bound.[31] It is binding at the high affinity site that drives the ligand-induced structure-switching binding mechanism.

Despite widespread adoption of the cocaine binding aptamer in biosensor development, there has yet been no systematic analysis of the effect of changing the length of stem 1 on the ligand-induced structure-switching binding mechanism. In this study, we vary the length of stem 1 of the cocaine-binding aptamer from 1 to 7 base pairs (Figure 1) and evaluate how progressively changing stem 1 length affects the structure, thermal stability, and ligand-binding ability of the aptamer. We establish that the different binding affinity for cocaine and quinine can be used to fold and bind a cocaine-binding aptamer that has been destabilized from the typically studied 3-base-pair-long stem 1 to one being 2-base-pairs-long. Quinine binds with enough free energy to fold and bind the 2-base-pair-long aptamer, but cocaine does not bind with enough free energy to do the same. Additionally, we show that the cocaine-binding aptamer transitions from unfolded to folded in the free state when going from a 3- to a 4-base-pair-long stem 1. As the cocaine-binding aptamer is one of the most widely utilized aptameric probes in the biosensing field, the information presented in this study provides valuable insight into the best choice of cocaine-binding aptamer variant for use in biosensor development.

MATERIALS AND METHODS

Materials. All aptamer samples (Figure 1) were obtained from Integrated DNA Technologies (IDT). DNA samples were dissolved in distilled deionized H_2O (ddH_2O) and then exchanged three times using a 3 kDa molecular weight cut-off concentrator with sterilized 1 M NaCl followed by three exchanges into ddH_2O. In determining which sequences to investigate we used MN4 as a starting point and simply shortened the length of stem 1 one base pair at a time. In lengthening stem 1, we added a GC base pair in order to help maximize the stability of the longer stem 1 aptamer (OR11). Aptamer and ligand concentrations were determined by UV absorbance spectroscopy using the extinction coefficients supplied by the manufacturer. Cocaine hydrochloride and quinine hemisulfate monohydrate were obtained from Sigma-Aldrich.

NMR Spectroscopy. NMR experiments on aptamer samples were performed using a 600 MHz Bruker Avance spectrometer equipped with a $^{1}H-^{13}C-^{15}N$ triple-resonance probe and magnetic field gradients. All NMR spectra were acquired in $H_2O/^{2}H_2O$ (90%/10%) at 5 °C. Water suppression was achieved through the use of the WATERGATE sequence.[32] Aptamer concentrations for NMR studies were 0.2 mM.

Isothermal Titration Calorimetry. For isothermal titration calorimetry (ITC) experiments, DNA samples were exchanged into a buffer containing 20 mM Tris (pH 7.4 at room temperature), 140 mM NaCl, 5 mM KCl three times before use. These sample conditions match that of our previous studies and are those in which the cocaine-binding aptamer was selected.[15,16,28] ITC experiments were performed using a MicroCal VP-ITC instrument. Data were fit to a one-site binding model using Origin 7 software. Samples were degassed prior to analysis using the MicroCal ThermoVac unit. All experiments were acquired at 10 °C and corrected for the heat of dilution of the titrant. Cocaine and quinine solutions were prepared in the same buffer as the DNA aptamer. Cocaine binding experiments were performed with an aptamer solution of 70 μM using a ligand concentration of 1.1 mM. Quinine binding experiments were performed with an aptamer solution of 20 μM using a ligand concentration of 0.312 mM. All titrations were performed with the aptamer in the cell and the ligand in the syringe. All aptamer samples were heated in a boiling water bath for 3 min and cooled in an ice bath preceding ITC experiments to allow the aptamer to anneal. Binding experiments consisted of 35 successive 8 μL injections spaced every 300 s, where the first injection was 2 μL to account for diffusion from the syringe into the cell.

UV and Differential Scanning Fluorimetry Melts. UV thermal melt experiments were performed using a Cary 100 spectrometer and 10 mm fused quartz cuvettes. The DNA melting curves were observed in a temperature range of 5 to 80 °C for quinine-aptamer assays. The temperature was changed throughout each experiment at 1 °C min^{-1} using a Cary Peltier controller. Each experiment was performed in 20 mM sodium phosphate buffer (pH 7.4), 140 mM NaCl. For each run, a concentration of aptamer was chosen to yield ~0.5 absorbance arbitrary units (a.u.) at 260 nm using the known extinction coefficients of the aptamer. For aptamer-quinine complexes, the amount of ligand was adjusted to provide a 95% ligand-bound aptamer sample based on the known K_d values. The observed UV light absorbance at 260 nm from 4 to 6 replicates was averaged and then the difference between the average sample and average blank absorbance was obtained. For free aptamer, the blank was the corresponding buffer; for aptamer-quinine samples, the blank was quinine in the buffer used. This difference was then normalized as $(\Delta I_{max} - \Delta I_i)/(\Delta I_{max} - \Delta I_{min})$ where ΔI_{max} is the maximum value of the difference between the sample absorbance, ΔI_{min} is the minimum value of the difference between the sample absorbance, and ΔI_i is the value of the difference between the sample and blank absorbance at a particular temperature. Then the normalized absorbance was plotted against the temperature.

DOI: 10.1021/acssensors.7b00619
ACS Sens. 2017, 2, 1539−1545

To quantify the T_m value, the first derivative of each thermal curve was plotted as a function of temperature using OriginPro 2016 Software.

Fluorescence thermal shift assays were performed employing a 90°-light path Cary Eclipse spectrofluorometer and 10 mm fused quartz cuvettes. The temperature was monitored throughout each experiment at 1 °C min^{-1} using a Cary Peltier controller. The thermal shifts were observed in the same temperature range, buffer, and ligand:aptamer molar ratios as used for the UV melts. Quinine-aptamer complexes were optimized for the excitation and emission maxima of quinine, photomultiplier tube voltage, signal-to-noise ratio, and spectral bandwidth parameters. The observed fluorescence emission intensities from 4 to 6 replicates were corrected for the inner-filter effect to compensate for the loss of the light intensity by the aptamer.[33,34] The obtained corrected fluorescence intensities were averaged then normalized as described above for the UV melts. In the assays of the quinine-aptamer complexes, quinine was excited at 234 and 332 nm, and the emission maxima were recorded at 386 nm.

RESULTS AND DISCUSSION

NMR Spectroscopy of the Cocaine-Binding Aptamers with Varying Stem 1 Length. NMR spectroscopy was performed in order to see how the structure of the aptamer changes as the length of stem 1 increases. Figure 2 shows the 1D ^{1}H NMR spectra of the imino region of the unbound aptamers with 2 to 7 base pairs in stem 1. Assignments are based on our previously reported spectra of MN4.[15,28] The spectrum of MN4 reported here matches that reported earlier except for some small changes in chemical shift for T18.

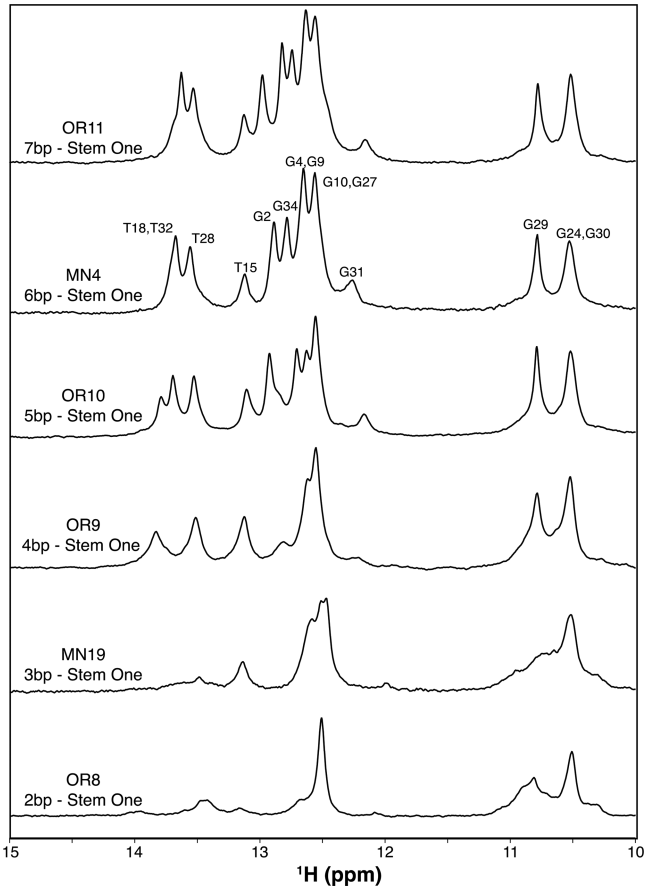

Figure 2. 1D ^{1}H NMR spectra of the aptamers used in this study. Displayed is the region of the NMR spectrum focusing on the imino resonances of the ligand-free aptamers. All spectra were acquired in 90% H_2O/10% ^2H_2O at 5 °C.

Similarly, the spectrum of MN19 resembles what we have previously reported.[28] From a qualitative analysis of the spectra of the 6 aptamers, we note that all the expected peaks are present, and the peaks are sharpest for the constructs containing 4 and more base pairs in stem 1 (OR9, OR10, MN4, and OR11; Figure 2). For the aptamer constructs with 2 and 3 base pairs in stem 1, OR8 and MN19, the signals are noticeably broader and fewer peaks are observed for the number of imino resonances expected in the predicted secondary structure. For example, the peak from G31, which is the resonance that changes shift the most with both cocaine and quinine binding, is not identifiable in the aptamer variants with 2 and 3 base pairs. However, it is clearly visible in constructs with 4 base pairs or more. The relative sharpness of the peaks in the spectra of the aptamers with 4 or more base pairs in stem 1 indicate that these constructs are tightly structured with all three stems being formed. For aptamers MN19 and OR8, the broad peaks are indicative of these molecules being more dynamic or poorly structured. The presence of some imino protons in both MN19 and OR8 does show that these aptamers do contain at least partially formed stems.

The nature of the structure of the destabilized/unstructured free state (or ensemble of unstructured states) for OR8 and MN19 is not precisely known. Cekan et al. have proposed a model for a 3-base-pair stem 1 aptamer, where stems 2 and 3 are folded and stem 1 is not formed in the absence of ligand.[35] This model fits with our NMR data that shows the presence of a limited set of imino protons present in MN19 and OR8 (Figure 2). Due to a lack of cross peaks in 2D experiments for free MN19 we are unable to unambiguously assign these imino protons, but from analyzing the titration data the imino protons in free MN19 likely arise from base pairs in stems 2 and 3. It is not possible, solely on the basis of the NMR spectra, to discount the possibility that the free OR8 and MN19 have all base pairs formed, but that many imino protons are not observable in the NMR spectra due to rapid hydrogen exchange with bulk water due to the flexible or dynamic nature of these short stem 1 molecules. We have shown that ligand binding does reduce imino hydrogen exchange rates at nucleotides near the binding site.[17] Whatever is structurally occurring in the free OR8 and MN19, it is clear that ligand-binding results in a dramatically better-structured or ordered aptamer.

Thermal Stability of the Stem 1 Constructs. We have analyzed the stability of the free and quinine-bound aptamers using UV-based thermal melts as well as using differential scanning fluorimetry thermal shift analysis for the quinine-bound aptamers. For free OR8 and MN19 the UV melts were straight lines, not sigmoidal, providing no evidence for the presence of a folded unbound aptamer (Figure 3a). This confirms the findings from the 1D NMR spectra of the aptamers that also provided no evidence for a fully folded unbound OR8 or MN19 aptamer.

When bound to quinine the aptamers with stem 1 two to seven base pairs long showed a sigmoidal denaturation curve (Figure 3b) with T_m values provided in Table 1. These values showed that as stem 1 progressively lengthened, the T_m values also progressively increased. These UV melts were confirmed using a fluorimetry based thermal shift assay looking at the quinine ligand being released from the bound aptamer (Figure 3c). Binding of aptamer quenches the intrinsic fluorescence of quinine.[36] Both the UV and fluorimetry-based thermal melting experiments match within the error range. In all of the aptamers

DOI: 10.1021/acssensors.7b00619
ACS Sens. 2017, 2, 1539−1545

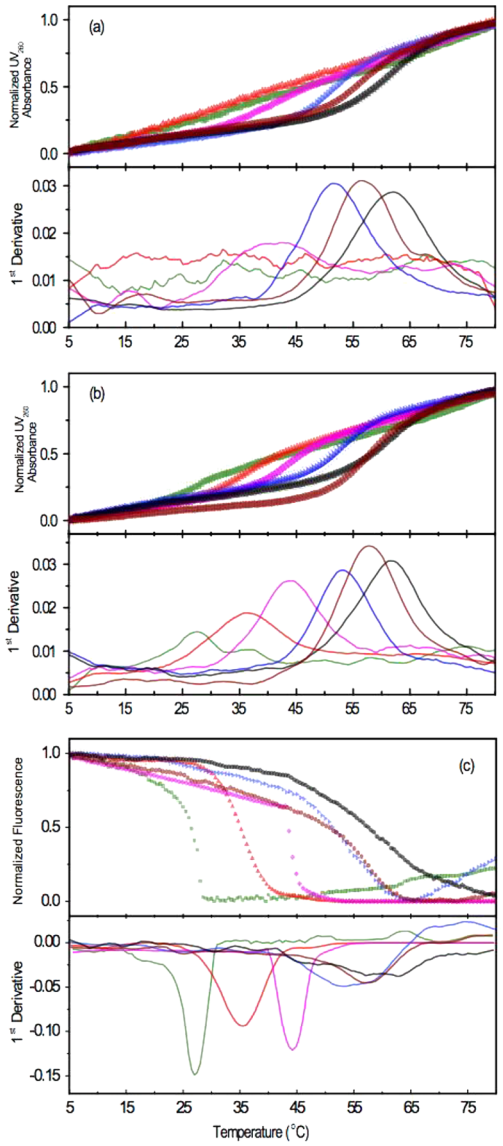

Figure 3. Analysis of the thermal stability of the unbound and quinine-bound aptamer constructs. Shown are the normalized UV absorbance at 260 nm for the OR8 (green), MN19 (red), OR9 (magenta), OR10 (blue), MN4 (brown), and OR11 (black) aptamer constructs: (a) unbound and (b) quinine-bound. Analysis of the thermal stability of the aptamer-quinine complexes using differential scanning fluorimetry thermal shift analysis is shown in (c). Each data point denotes an average of 4−6 experiments with the error bars corresponding to 1 standard deviation. Data acquired in 20 mM sodium phosphate buffer (pH 7.4), 140 mM NaCl.

analyzed, the T_m value of the quinine-bound aptamer is higher than that of the free aptamer. This indicates that ligand binding is occurring and that quinine binding stabilizes the structure of the aptamer.

Binding Affinity and Thermodynamics of the Cocaine-Binding Aptamer with Varying Stem 1 Length. ITC was used to analyze the functionality of the cocaine-binding aptamer as the length of stem 1 was varied between 2 and 7 base pairs long. With cocaine as a ligand, we observed binding for aptamers with a length of 3 base pairs or longer, and we detected no binding for OR8 (Figure 4a; Table 2). The nonobservation of cocaine binding by OR8 was confirmed by ITC performed under low-c conditions, 70 μM OR8 adding a 20-fold molar excess of cocaine. We observed no evidence for cocaine-binding (SI Figure 1). Additionally, a fluorescence-based titration of cocaine with the OR8 aptamer monitoring the intrinsic fluorescence of cocaine[36] also revealed no evidence of OR8 binding cocaine (SI Figure 2). As summarized in Table 2, the affinity of MN19 (3 base pairs) for cocaine is significantly lower than that of aptamers with a stem 1 longer than 3 base pairs and the affinity plateaus with 4 base pairs or more. Our binding affinities presented here, for both cocaine and quinine, match our previously reported data for both MN4 and MN19 within the error range and at the same temperature.[15,28,29,37]

With quinine as a ligand, we observed binding for the constructs with a stem 1 containing 2 or more base pairs (Figure 4b; Table 3). In contrast with cocaine, the two-base-pair aptamer (OR8) binds quinine. We also analyzed quinine binding to a construct containing 1 base pair (OR7), but we only observed very weak binding in the millimolar range. Due to the low affinity, we were unable to reliably analyze the binding for this construct with ITC. The affinity for quinine significantly increases when stem 1 lengthens from 2 to 3 base pairs. However, for aptamer constructs 3 base pairs and longer the affinities are all within the reported error range.

From the binding enthalpy and entropy we see that the aptamer-ligand pairs that undergo the structure switching mechanism (MN19-quinine, OR8-quinine, MN19-cocaine) display the most unfavorable ($-T\Delta S$) values and generally have the most exothermic binding enthalpy values. The easiest explanation for these findings is that more hydrogen bonds form with structure formation leading to a more negative ΔH for binding and that there is a greater entropy penalty to pay for a transition from an unbound and poorly structured aptamer to a bound folded aptamer than from an unbound well-structured aptamer to a bound folded aptamer. However, caution must be used in making these arguments as other factors such as solvation also play a part in the binding mechanism.

Table 1. Melt Temperature of the Different Aptamer Constructs Determined Using UV Absorbance and Differential Fluorimetry Thermal Shift Assays[1]

aptamer	free (°C)	quinine-bound (UV) (°C)	quinine-bound (fluorimetry) (°C)
OR8	N/A	28 ± 1	27.0 ± 0.9
MN19	N/A	35.6 ± 0.3	35.2 ± 0.5
OR9	42.6 ± 0.6	44.1 ± 0.4	44.2 ± 0.7
OR10	51.6 ± 0.4	53.1 ± 0.4	53.1 ± 0.6
MN4	56.7 ± 0.4	57.6 ± 0.4	57.6 ± 0.5
OR11	61.7 ± 0.6	62.1 ± 0.2	62.6 ± 0.3

[a]Data acquired in 20 mM sodium phosphate (pH 7.4), 140 mM NaCl. The values reported are averages of 4−6 individual experiments. N/A denotes no melt detected.

DOI: 10.1021/acssensors.7b00619
ACS Sens. 2017, 2, 1539−1545

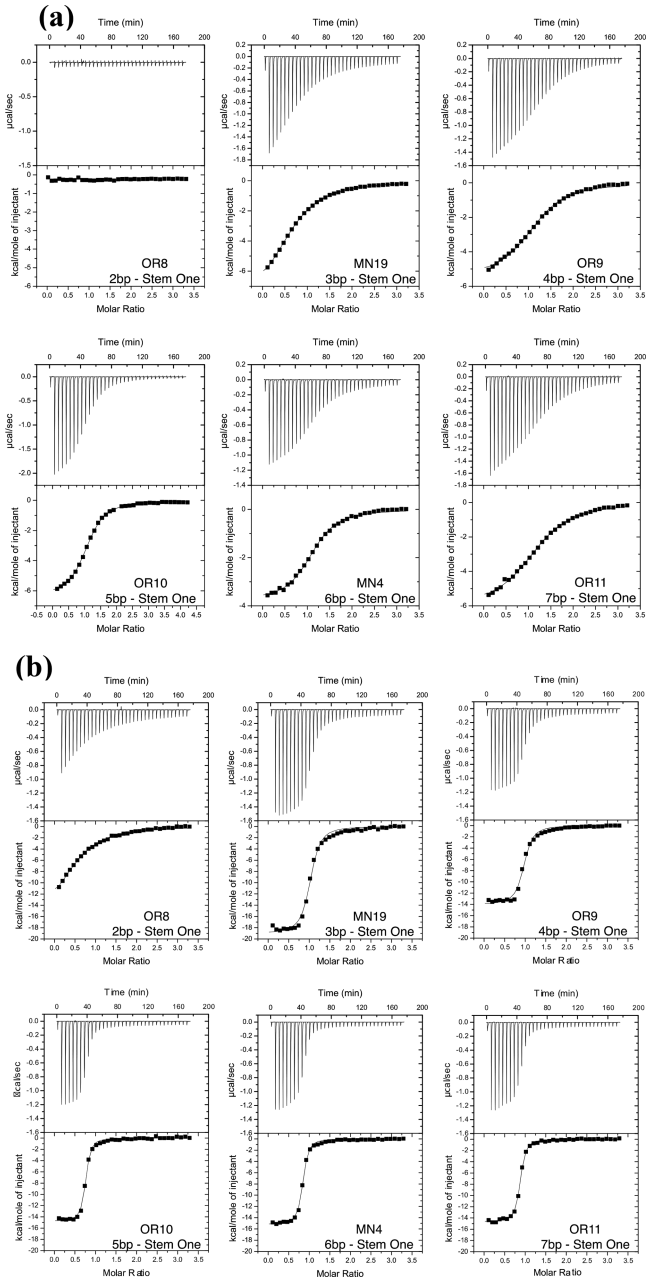

Figure 4. ITC data showing the interaction of the different stem 1 length aptamers with (a) cocaine and (b) quinine. On top is the raw titration data showing the heat resulting from each injection of ligand into aptamer solution. The bottom shows the integrated heat plot after correcting for the heat of dilution. Data were acquired in 20 mM Tris (pH 7.4), 140 mM NaCl, 5 mM KCl.

CONCLUSION

Our results presented here support a general mechanism where it is possible to destabilize an aptamer in order to improve ligand selectivity for tighter binding ligands. This improved selectivity does come at the price of a reduced affinity for the new aptamer-ligand pairing. In a previous study we did the reverse process and increased the stability of an aptamer by adding a base pair to the deoxycholic acid steroid-binding aptamer.[38] This more stable aptamer, a single base pair longer in the terminal stem, was still unfolded while free and became structured with ligand binding. This increase in the stability of the free, but still unfolded, aptamer was needed due to the weak

Table 2. Affinity and Thermodynamic Parameters of Cocaine Binding by the Aptamers Used in This Study[1]

aptamer	K_d (μM)	ΔH (kcal/mol)	$-T\Delta S$ (kcal/mol)	ΔG (kcal/mol)
OR7 (1 bp)		nbd		
OR8 (2 bp)		nbd		
MN19 (3 bp)	17 ± 3	−8.6 ± 0.4	−2.3 ± 0.2	−6.3 ± 0.6
OR9 (4 bp)	9.5 ± 0.2	−7.3 ± 0.3	−0.8 ± 0.4	−6.5 ± 0.7
OR10 (5 bp)	7.0 ± 0.3	−6.3 ± 0.2	4.7 ± 0.2	−6.7 ± 0.1
MN4 (6 bp)	8.6 ± 4.4	−4.3 ± 0.7	2.4 ± 0.8	−6.7 ± 0.1
OR11 (7 bp)	9.8 ± 2.8	−4.9 ± 0.2	1.5 ± 0.5	−6.4 ± 0.3

[a]Data acquired at 10 °C in 20 mM Tris (pH 7.4), 140 mM NaCl, 5 mM KCl. The values reported are averages of 2 to 6 individual experiments. nbd denotes no binding detected.

Table 3. Affinity and Thermodynamic Parameters of Quinine Binding by the Aptamers Used in This Study[1]

aptamer	K_d (μM)	ΔH (kcal/mol)	$-T\Delta S$ (kcal/mol)	ΔG (kcal/mol)
OR7 (1 bp)	vwb	vwb	vwb	vwb
OR8 (2 bp)	11.2 ± 0.5	−15 ± 2	8.4 ± 1.7	−6.5 ± 0.3
MN19 (3 bp)	0.23 ± 0.09	−18.6 ± 0.7	10.0 ± 0.9	−8.6 ± 0.2
OR9 (4 bp)	0.21 ± 0.06	−14.2 ± 0.2	5.5 ± 0.1	−8.7 ± 0.2
OR10 (5 bp)	0.13 ± 0.04	−15.1 ± 0.5	6.2 ± 0.6	−8.9 ± 0.2
MN4 (6 bp)	0.15 ± 0.06	−14.6 ± 0.9	5.7 ± 0.7	−8.9 ± 0.2
OR11(7 bp)	0.14 ± 0.07	−14.9 ± 0.4	6.0 ± 0.6	−8.9 ± 0.3

[a]Data acquired at 10 °C in 20 mM Tris (pH 7.4), 140 mM NaCl, 5 mM KCl. The values reported are averages of 2 to 3 individual experiments. vwb denotes that only very weak (mM) binding is observed.

binding by the ligand (~15 μM) and consequently smaller amount of free energy available to contribute to folding.

We propose a free energy diagram as shown in Figure 5 to help explain our results reported here. For OR8 and MN19 the

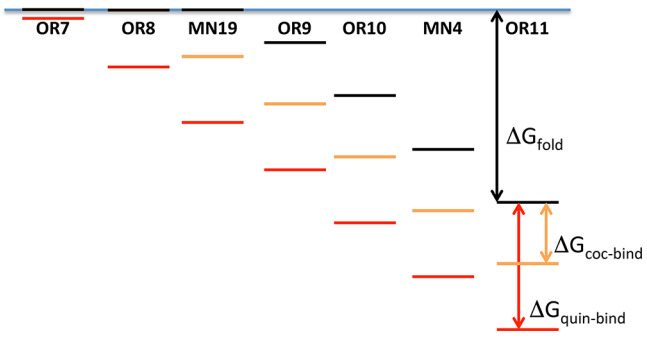

Figure 5. Free energy diagram outlining the binding scheme observed for the cocaine-binding aptamer with a varying stem 1 length. The blue line indicates the level below which the aptamer or aptamer-ligand complex folds. The relative energy levels of unfolded states are not indicated.

unbound state is below the threshold for a fully structured aptamer whereas the free aptamer is folded for aptamers with a stem 1 four base pairs and longer. The free energy of quinine binding is greater than that of cocaine binding as manifested in the tighter binding of quinine compared to cocaine. We also assume that the binding of a ligand interacts roughly equally

DOI: 10.1021/acssensors.7b00619
ACS Sens. 2017, 2, 1539−1545

with each folded unbound aptamer. This is shown by the ΔG of quinine and cocaine binding being within the error range for the aptamers OR9, OR10, MN4, and OR11 (Tables 2 and 3). Additionally, the difference in the unbound free energy of OR9 to OR11 is roughly equal since they all differ by one GC base pair. We conclude that the binding free energy supplied by quinine is enough to fold the OR8 and MN19 aptamer constructs, but cocaine binding only supplies enough free energy to fold MN19 and not the less stable OR8. This implies that more free energy is required to fold OR8 than to fold MN19. For OR8, the free energy supplied by quinine binding is enough to fold the aptamer and supply an apparent K_d of (11.2 ± 0.5) μM. In contrast, the ΔG supplied by cocaine binding is not enough to fold this aptamer and no binding is observed. For MN19, the ΔG supplied by both quinine and cocaine are enough to fold the aptamer with the excess amount resulting in the apparent K_d value. The results provided here should provide a direction for the development of surface-sensitive sensor techniques using the cocaine-binding aptamer. The use of an aptamer with 2 base pairs in stem 1, such as OR8, may provide a more sensitive sensor when using quinine as an analyte than the 3-base-pair-long MN19, as it may transition from a more unfolded unbound state.

■ ASSOCIATED CONTENT

Supporting Information

The Supporting Information is available free of charge on the ACS Publications website at DOI: 10.1021/acssensors.7b00619.

Figures S1 and S2 showing no evidence for the interaction of OR8 and cocaine (PDF)

■ AUTHOR INFORMATION

Corresponding Author

*E-mail: pjohnson@yorku.ca. Phone: 416-736-2100 x3319.

ORCID

Philip E. Johnson: 0000-0002-5573-4891

Author Contributions

‡M.A.D.N., A.A.S., and O.R. contributed equally to this work.

Notes

The authors declare no competing financial interest.

■ ACKNOWLEDGMENTS

This work was supported by funding from the Natural Sciences and Engineering Research Council of Canada (NSERC) to P.E.J. We thank Logan Donaldson (York University) for the use of his spectrofluorometer as well as past and present lab members for useful discussions.

■ REFERENCES

(1) Li, D.; Song, S.; Fan, C. Target-responsive structural switching for nucleic acid-based sensors. *Acc. Chem. Res.* **2010**, *43*, 631−641.

(2) Schoukroun-Barnes, L. R.; Macazo, F. C.; Gutierrez, B.; Lottermoser, J.; Liu, J.; White, R. J. Reagentless, Structure-Switching, Electrochemical Aptamer-Based Sensors. *Annu. Rev. Anal. Chem.* **2016**, *9*, 163−181.

(3) Du, Y.; Dong, S. Nucleic Acid Biosensors: Recent Advances and Perspectives. *Anal. Chem.* **2017**, *89* (1), 189−215.

(4) Alsaafin, A.; McKeague, M. Functional nucleic acids as *in vivo* metabolite and ion biosensors. *Biosens. Bioelectron.* **2017**, *94*, 94−106.

(5) Nutiu, R.; Li, Y. Structure-Switching Signaling Aptamers: Transducing Molecular Recognition into Fluorescence Signaling. *Chem. - Eur. J.* **2004**, *10* (8), 1868−1876.

(6) Famulok, M.; Mayer, G. Aptamer modules as sensors and detectors. *Acc. Chem. Res.* **2011**, *44*, 1349−1358.

(7) Tang, Y.; Ge, B.; Sen, D.; Yu, H.-Z. Functional DNA switches: rational design and electrochemical signaling. *Chem. Soc. Rev.* **2014**, *43* (2), 518−529.

(8) Neves, M. A. D.; Blaszykowski, C.; Bokhari, S.; Thompson, M. Ultra-high frequency piezoelectric aptasensor for the label-free detection of cocaine. *Biosens. Bioelectron.* **2015**, *72*, 383−392.

(9) Neves, M. A. D.; Blaszykowski, C.; Thompson, M. Utilizing a Key Aptamer Structure-Switching Mechanism for the Ultrahigh Frequency Detection of Cocaine. *Anal. Chem.* **2016**, *88*, 3098−3106.

(10) Liu, J.; Lu, Y. Fast colorimetric sensing of adenosine and cocaine based on a general sensor design involving aptamers and nanoparticles. *Angew. Chem., Int. Ed.* **2006**, *45*, 90−94.

(11) Baker, B. R.; Lai, R. Y.; Wood, M. S.; Doctor, E. H.; Heeger, A. J.; Plaxco, K. W. An electronic, aptamer-based small-molecule sensor for the rapid, label-free detection of cocaine in adulterated samples and biological fluids. *J. Am. Chem. Soc.* **2006**, *128*, 3138−3139.

(12) Swensen, J. S.; Xiao, Y.; Ferguson, B. S.; Lubin, A. A.; Lai, R. Y.; Heeger, A. J.; Plaxco, K. W.; Soh, H. T. Continuous, real-time monitoring of cocaine in undiluted blood serum via a microfluidic, electrochemical aptamer-based sensor. *J. Am. Chem. Soc.* **2009**, *131*, 4262−4266.

(13) Kawano, R.; Osaki, T.; Sasaki, H.; Takinoue, M.; Yoshizawa, S.; Takeuchi, S. Rapid detection of a cocaine-binding aptamer using biological nanopores on a chip. *J. Am. Chem. Soc.* **2011**, *133*, 8474−8477.

(14) Das, J.; Cederquist, K. B.; Zaragoza, A. A.; Lee, P. E.; Sargent, E. H.; Kelley, S. O. An ultrasensitive universal detector based on neutralizer displacement. *Nat. Chem.* **2012**, *4*, 642−648.

(15) Neves, M. A. D.; Reinstein, O.; Johnson, P. E. Defining a stem length-dependant binding mechanism for the cocaine-binding aptamer. A combined NMR and calorimetry study. *Biochemistry* **2010**, *49*, 8478−8487.

(16) Stojanovic, M. N.; de Prada, P.; Landry, D. W. Aptamer-based folding fluorescent sensor for cocaine. *J. Am. Chem. Soc.* **2001**, *123*, 4928−4931.

(17) Churcher, Z. R.; Neves, M. A. D.; Hunter, H. N.; Johnson, P. E. Comparison of the free and ligand-bound imino hydrogen exchange rates for the cocaine-binding aptamer. *J. Biomol. NMR* **2017**, *68*, 33−39.

(18) Sugase, K.; Dyson, H. J.; Wright, P. E. Mechanism of coupled folding and binding of an intrinsically disordered protein. *Nature* **2007**, *447* (7147), 1021−1025.

(19) van der Lee, R.; Buljan, M.; Lang, B.; Weatheritt, R. J.; Daughdrill, G. W.; Dunker, A. K.; Fuxreiter, M.; Gough, J.; Gsponer, J.; Jones, D. T.; Kim, P. M.; Kriwacki, R. W.; Oldfield, C. J.; Pappu, R. V.; Tompa, P.; Uversky, V. N.; Wright, P. E.; Babu, M. M. Classification of Intrinsically Disordered Regions and Proteins. *Chem. Rev.* **2014**, *114* (13), 6589−6631.

(20) Shammas, S. L.; Crabtree, M. D.; Dahal, L.; Wicky, B. I. M.; Clarke, J. Insights into Coupled Folding and Binding Mechanisms from Kinetic Studies. *J. Biol. Chem.* **2016**, *291* (13), 6689−6695.

(21) Li, Y.; Qi, H.; Peng, Y.; Yang, J.; Zhang, C. Electrogenerated chemiluminescence aptamer-based biosensor for the determination of cocaine. *Electrochem. Commun.* **2007**, *9* (10), 2571−2575.

(22) Li, T.; Li, B.; Dong, S. Adaptive recognition of small molecules by nucleic acid aptamers through a label-free approach. *Chem. - Eur. J.* **2007**, *13*, 6718−6723.

(23) Chen, J.; Jiang, J.; Gao, X.; Liu, G.; Shen, G.; Yu, G. A new aptameric biosensor for cocaine based on surace-enhanced raman scattering spectroscopy. *Chem. - Eur. J.* **2008**, *14*, 8374−8382.

(24) Abelow, A. E.; Schepelina, O.; White, R. J.; Vallee-Belisle, A.; Plaxco, K. W.; Zharov, I. Biomimetic glass nanopores employing aptamer gates responsive to a small molecule. *Chem. Commun.* **2010**, *46* (42), 7984−7986.

DOI: 10.1021/acssensors.7b00619
ACS Sens. 2017, 2, 1539−1545

(25) Hu, X.; Mu, L.; Zhou, Q.; Wen, J.; Pawliszyn, J. ssDNA aptamer-based column for simultaneous removal of nanogram per liter level of illicit and analgesic pharmaceuticals in drinking water. *Environ. Sci. Technol.* **2011**, *45*, 4890−4895.
(26) Malile, B.; Chen, J. I. Morphology-based plasmonic nanoparticle sensors: controlling etching kinetics with target-responsive permeability gate. *J. Am. Chem. Soc.* **2013**, *135*, 16042−16045.
(27) Pei, R.; Shen, A.; Olah, M. J.; Stefanovic, D.; Worgall, T.; Stojanovic, M. N. High-resolution cross-reactive array for alkaloids. *Chem. Commun.* **2009**, 3193−3195.
(28) Reinstein, O.; Yoo, M.; Han, C.; Palmo, T.; Beckham, S. A.; Wilce, M. C. J.; Johnson, P. E. Quinine binding by the cocaine-binding aptamer. Thermodynamic and hydrodynamic analysis of high-affinity binding of an off-target ligand. *Biochemistry* **2013**, *52*, 8652−8662.
(29) Slavkovic, S.; Altunisik, M.; Reinstein, O.; Johnson, P. E. Structure-affinity relationship of the cocaine-binding aptamer with quinine derivatives. *Bioorg. Med. Chem.* **2015**, *23*, 2593−2597.
(30) Harkness, R. W.; Slavkovic, S.; Johnson, P. E.; Mittermaier, A. K. Rapid characterization of folding and binding interactions with thermolabile ligands by DSC. *Chem. Commun.* **2016**, *52* (92), 13471−13474.
(31) Neves, M. A. D.; Slavkovic, S.; Churcher, Z. R.; Johnson, P. E. Salt-mediated two-site ligand binding by the cocaine-binding aptamer. *Nucleic Acids Res.* **2017**, *45*, 1041−1048.
(32) Piotto, M.; Saudek, V.; Sklenar, V. Gradient-tailored excitation for single-quantum NMR spectroscopy of aqueous solutions. *J. Biomol. NMR* **1992**, *2*, 661−665.
(33) Van De Weert, M. Fluorescence quenching to study protein-ligand binding: Common errors. *J. Fluoresc.* **2010**, *20* (2), 625−629.
(34) Van De Weert, M.; Stella, L. Fluorescence quenching and ligand binding: A critical discussion of a popular methodology. *J. Mol. Struct.* **2011**, *998* (1−3), 145−150.
(35) Cekan, P.; Jonsson, E. O.; Sigurdsson, S. T. Folding of the cocaine aptamer studied by EPR and fluorescence spectroscopies using the bifunctional spectroscopic probe Ç. *Nucleic Acids Res.* **2009**, *37*, 3990−3995.
(36) Shoara, A. A.; Slavkovic, S.; Donaldson, L. W.; Johnson, P. E. Analysis of the Interaction between the Cocaine-Binding Aptamer and its Ligands using Fluorescence Spectroscopy. *Can. J. Chem.* **2017**, 1 DOI: 10.1139/cjc-2017-0380.
(37) Neves, M. A. D.; Reinstein, O.; Saad, M.; Johnson, P. E. Defining the secondary structural requirements of a cocaine-binding aptamer by a thermodynamic and mutation study. *Biophys. Chem.* **2010**, *153*, 9−16.
(38) Reinstein, O.; Neves, M. A. D.; Saad, M.; Boodram, S. N.; Lombardo, S.; Beckham, S. A.; Brouwer, J.; Audette, G. F.; Groves, P.; Wilce, M. C. J.; Johnson, P. E. Engineering a structure switching mechanism into a steroid binding aptamer and hydrodynamic analysis of the ligand binding mechanism. *Biochemistry* **2011**, *50*, 9368−9376.

DOI: 10.1021/acssensors.7b00619
ACS Sens. 2017, 2, 1539−1545